

Research Article

# A Multi-Scale Finite Element Model of Bruising in Soft Connective Tissues

Lu Huang,<sup>2</sup> Noah Bakker,<sup>1</sup> James Kim,<sup>1</sup> Jez Marston,<sup>1</sup> Ian Grosse,<sup>2</sup> John Tis,<sup>3</sup> and Dennis Cullinane<sup>1</sup>

<sup>1</sup>Biomechanics Laboratory, Deerfield Academy, Deerfield, MA 01342, USA

<sup>2</sup>Department of Mechanical and Industrial Engineering, University of Massachusetts, Amherst, MA 01003, USA

<sup>3</sup>Department of Orthopaedic Surgery, School of Medicine, Johns Hopkins University, Baltimore, MD 21287, USA

Address correspondence to Dennis Cullinane, dcullinane@deerfield.edu

Received 16 May 2012; Revised 31 July 2012; Accepted 11 October 2012

**Abstract** The failure of capillaries, or bruising, is a common physical exam finding following blunt trauma, and can be indicative of intentional trauma and abuse. However, despite the obvious clinical and forensic applications, there exist no computer models of bruising in soft connective tissues. We generated a finite element model of an adult female human arm segment, including skin, adipose, skeletal muscle, and bone, to determine the relationship between applied load, and the stresses and strains experienced by the tissue layers when impacted by a punch. The maximum principal stress in the wall of the capillary was 89.6 kPa, indicating that bruising would likely result in the skin, adipose, and skeletal muscle under these specific loading conditions, and that bruising is not limited to the impact site. The determination of bruise etiology has implications for forensic analyses and clinical procedures, and may have specific uses in characterizing abuse trauma.

**Keywords** capillary failure; finite element analysis; bruising

## 1 Introduction

A bruise is an area of closed hemorrhage into soft tissue due to the rupture of blood vessels caused by blunt trauma [16] or pressure differentials [19]. A bruise is typically present in soft connective tissues such as skin, adipose and muscle, as well as bone, but can also present clinically in internal organs such as the lungs [17], heart [3], and brain [8]. When forces impact soft tissues, they deform relative to the load magnitude, anatomical location, rate of loading, and load orientation; and when the ultimate stress of the tissue is reached, the tissue fails [4]. This occurs in bruising, when the applied stress overcomes the maximum tensile strength of the capillaries, they rupture, and blood is released into the soft tissues. There are three common types of bruising: subcutaneous, intramuscular and periosteal. Subcutaneous bruises are limited to the skin and adipose tissue, whereas intramuscular and periosteal bruises describe those found

in the skeletal muscle and bone, respectively. Subcutaneous bruising requires that skin not experience tearing; however, intramuscular or periosteal bruising may be accompanied by tearing of the skin [11].

Bruising is a common medical condition and it can result from accidental trauma, but its presence may also imply intentional trauma, as in cases of intimate partner violence or child abuse. For example, soft tissue injuries were found in up to 92% of children suspected of being victims of child abuse [2]. Bruises in specific anatomical locations can be indicative of intentional trauma; most commonly including the buttocks, perineum, trunk, posterior legs, posterior ribs, and the head or neck [2,7,9]. Despite such practical implications, there have been no finite element model (FEM) studies that attempt to model bruising in soft connective tissues, while a few studies have used finite element analysis to model bruising in the brain [8] and the lungs [17]. Desmoulin and Anderson [6] created a kinetic model of bruising for living subjects that estimated energy absorbed and energy density upon impact, but that model was restricted to an estimate of surface forces. However, a finite element model that complements the work of Desmoulin and Anderson would go far towards validating a mechanical model of bruising, and vice versa.

Finite Element Analysis (FEA) is a numerical technique used to approximately solve partial differential equations of equilibrium that govern the stresses and strains that result when a model structure is loaded. The process involves the approximation of the physical geometry into a contiguous set of smaller, simply shaped entities called elements, connected together at points called nodes, forming a finite element mesh. Material properties are assigned to each element based on material test data, and appropriate kinematic constraints and loading conditions such as compression, tension, bending, and torsion are applied. The finite element model is then solved to obtain the elastic deformation of the structure, including the patterns and magnitudes of stresses

**Table 1:** Material properties of tissue layers values were taken from the biomechanical literature and incorporated into the model for each tissue layer. References for material property values are provided in brackets.

Tissue layer	Density ( $\text{kg/m}^3$ )	Young's modulus (MPa)	Poisson's ratio
Dermis and epidermis (skin) [5, 13]	$1.05 \times 10^{-6}$	0.035	0.48
Subcutaneous adipose [18]	$9.19 \times 10^{-7}$	0.244	0.49
Skeletal muscle [10, 18]	$1.06 \times 10^{-6}$	0.07	0.37
Capillary wall [1, 10]	$1.00 \times 10^{-6}$	0.37	0.495
Blood [15]	$1.06 \times 10^{-6}$	0.03	0.499

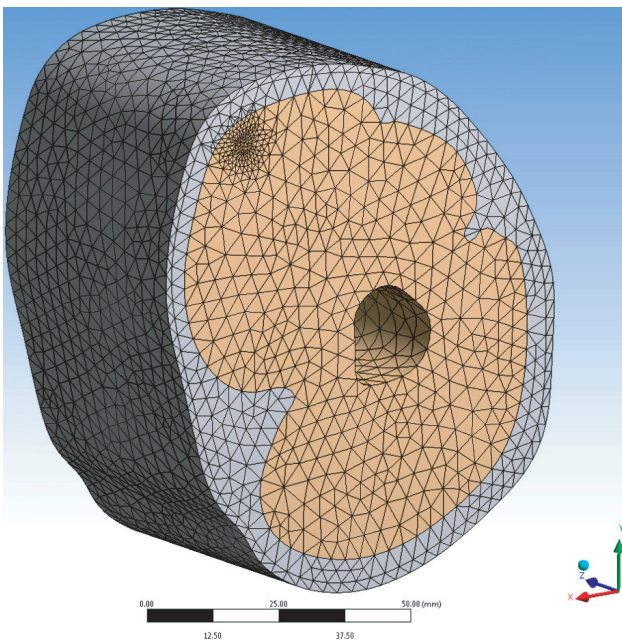


**Figure 1:** Global model of the arm section with a hollow cavity representing the humerus. Note the high density of elements in the top left resulting from the nested submodels.

and strains due to the applied loading conditions. Thus, the mechanical behavior of even complex structures can be simulated and failure thresholds estimated. This study investigated the impact of bruising on the human upper arm by simulating a traumatic, high-speed impact in order to characterize bruise etiology in soft connective tissues.

## 2 Materials and methods

### 2.1 Finite element analysis

A geometry model of the human upper arm was created in ANSYS Workbench 14.0 Design Modeler (Figure 1). To simplify the modeling process, the cross-section of an adult female arm was imported from the Visible Human Project using Solid Works, and subsequently imported as a geometry template into Design Modeler. The two-dimensional geometric face was extruded 100 mm to create

a longitudinally symmetrical arm segment which had a resulting diameter of 111 mm (major axis) and contained the three soft connective tissue layers: skin, subcutaneous adipose tissue, skeletal muscle, and bone as a scaffold. Three nested submodels were created with a capillary embedded in the final muscle submodel (Figure 1). Tissues were finalized by assigning appropriate material properties of density, Young's modulus, and Poisson's ratio, that were taken from the biomechanical literature (Table 1). Bone as a tissue was not considered in solving the model as it is orders of magnitude stiffer than the surrounding soft tissues, and thus, for the purposes of modeling soft connective tissue bruising, it was treated as a rigid mechanical framework. By neglecting fluid acceleration effects, we were able to model the blood within the capillary in the final capillary submodel as a nearly incompressible elastic solid to account for its incompressibility, precluding the need for a coupled structural-fluid mechanics simulation [21].

Because capillaries scale to microns and the arm segment scales to centimeters, the model utilized a multi-scale finite element submodeling approach consisting of a global finite element model of the upper arm with the sequence of three submodels, each of decreasing size. The global model representing the arm contained the three nested submodels of 4.0 mm, 0.2 mm, and 0.048 mm diameter volumes (submodels were necessary considering that the diameter of the global arm model is 14,000 times larger than a capillary). Contained within the smallest submodel was a single capillary of outer diameter 8 microns and wall thickness of 1 micron, and which was situated across the border of the applied load. The total volume of the global model was  $7.323 \times 10^5 \text{ mm}^3$ , with a mass of 0.7528 kg, and was constructed of 197,112 elements and 275,992 nodes. In the submodeling approach, a global finite model is solved to obtain the displacement field. Interpolation is used to map displacements found in the global model to displacements that act on the boundary of the submodel. Additional internal geometric details, which are too small to include in the global model, are then included in the submodel. The submodel is then solved and the process repeated if further submodels are needed.

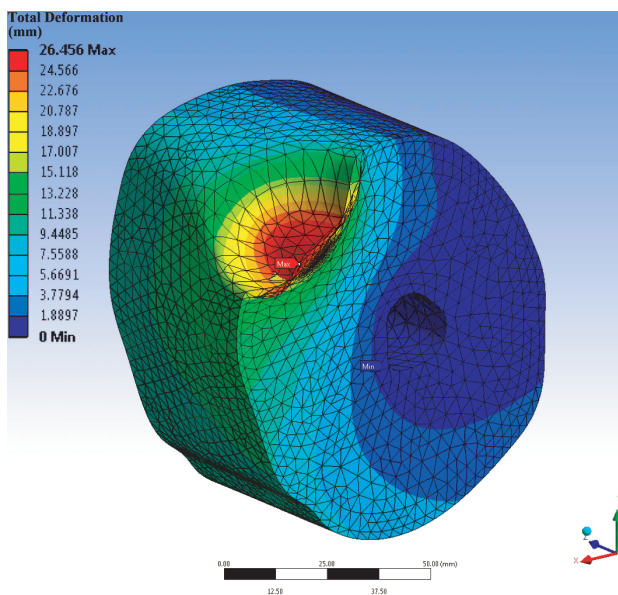


**Figure 2:** Peak total deformation of the global model experienced at time  $t = 0.044$  s due to transient pressure load.

A pressure with a peak magnitude of 0.1 MPa was applied to 648 mm<sup>2</sup> impact area on the surface of the skin over a time period of 0.06 s, reaching a peak pressure at 0.04 s, and subsequently returning to zero at 0.06 s. This combination of load and application rate was chosen to simulate a physiologically realistic impact to the center of the model, on a central axis perpendicular to the long axis of the humerus. For the transient upper-arm model, the density values of skin, adipose, and muscle tissue were taken from the literature, as indicated in Table 1. Because the global model is time dependent, the density of each material is a significant factor in the analysis. All submodels were necessarily static analyses based on peak time step results from the global model.

For the purposes of this study, it was assumed that bruising would be represented in the model by regions in which the maximum principal stress level surpassed the ultimate tensile stress of the capillary wall. We based this on the research by West et al. [1,19,20] who has extensively studied pulmonary capillary failure. Their research suggests that pulmonary capillary failure is due to hoop (i.e., circumferential) stresses in the capillary wall as a result of high transmural pressure which dilates the capillary. Based on simple biomechanical analysis and estimated transmural pressures that resulted in pulmonary capillary failure, they estimated a failure hoop stress of approximately 84 kPa. Since hoop stress also corresponds to the maximum principal stress in a hollow cylinder under internal pressure, the estimated hoop failure stress of 84 kPa represents the ultimate tensile strength of a pulmonary

capillary. We could find no work in the literature providing histological or biomechanical analysis of failure mechanism of capillaries in other tissues. We suggest that capillaries in other soft tissue, such as adipose and muscle, may fail by a similar mechanism due to tensile stresses that will occur in the capillary wall even when compressive loads are applied to the skin. Results do confirm the existence of large tensile hoop stresses within the capillary wall due to pressure loading on the skin.

### 3 Results and discussion

A multi-scale finite element model of a human upper arm with skin, subcutaneous adipose tissue, skeletal muscle, and an individual capillary was successfully created in ANSYS *Workbench* 14.0. Because the model was bilaterally symmetrical along its long axis and thus results in either direction were identical, only half the model appears in the figures. This also served to generate cross-sectional views of the model and impact zone. The solved model demonstrated multidimensional waves of pressure propagating depth-wise and circumferentially from the impact area, resulting in a substantial peak deformation (Figure 2). The global model experienced a peak deformation of 26.45 mm, which was focused in the skin and adipose, but dampened by the skeletal muscle layer (Figure 2). The equivalent stress of the model was 0.0329 MPa in the skin, 0.028 MPa in the adipose, and 0.0188 MPa in the skeletal muscle (Figure 3). Stress was distributed depth-wise to the humerus, with additional stress concentrations on the muscle border with the humerus, peaking at 0.0235 MPa (Figure 3). The volumetric region for the first-level sub-model clearly experienced high stresses below the impact epicenter, and distributed radially (Figure 4). Capillary wall results demonstrated a peak maximum principal stress level of 89.5 kPa, exceeding the stress level estimated to cause failure in pulmonary capillaries [20,21], and therefore leaking their contents into the interstitial fluids. The lateral margins of the capillary wall experienced high tensile hoop stresses of the order of 50–60 kPa (Figure 5). Thus, even though the skin experiences high compressive loads, the portions of the capillary embedded in the underlying muscle tissue experience high tensile stresses that can result in capillary failure consistent with previously published mechanisms of pulmonary capillary failure.

### 4 Conclusions

In our multi-scale set of finite element models, high tensile stress levels were found from the impact surface, deep to the border of the humerus, and thus within skin, adipose, and muscle tissues. The stress distribution found in the capillary submodel indicates that tensile stresses are distributed from the impact site and outward radially. These results clearly show that high tensile stress levels consistent with a bursting

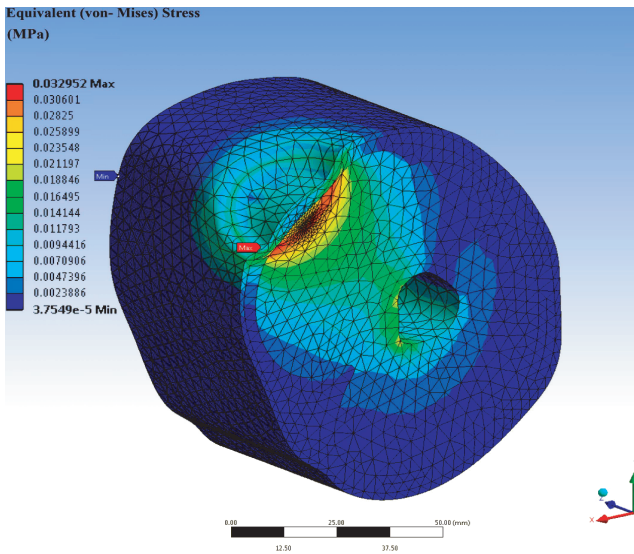


**Figure 3:** Equivalent (i.e., von Mises) stresses in the global model at time  $t = 0.044$  s.

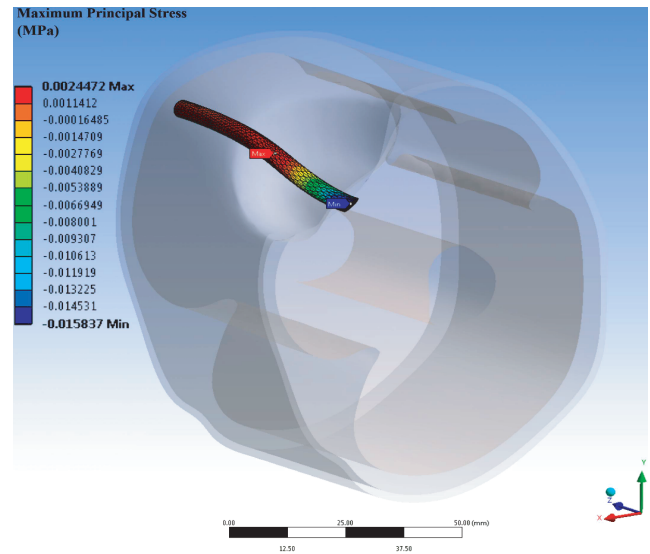


**Figure 4:** Maximum principal stresses in the volumetric region of the first level sub-model at time  $t = 0.044$  s.

capillary failure mechanism can be found in the muscle tissue within the area of impact, despite compressive loads applied to the skin, and that these high tensile stresses are the result of internal hydraulic pressure which produce high tensile hoop stresses in the capillary wall. The work of Tham et al. [19] supports the hypothesis that pressure differentials (increased internal pressure or reduced external pressure)

are the primary cause of capillary failure. It should also be noted that collagen, for example, is polyallelic and thus variation between individuals can be expected in both protein structure and mechanical properties [12, 14], and thus bruise thresholds. Future work is needed to confirm capillary failure mode and thus the etiology of bruising, as well as defining the load threshold window over which bruising occurs.

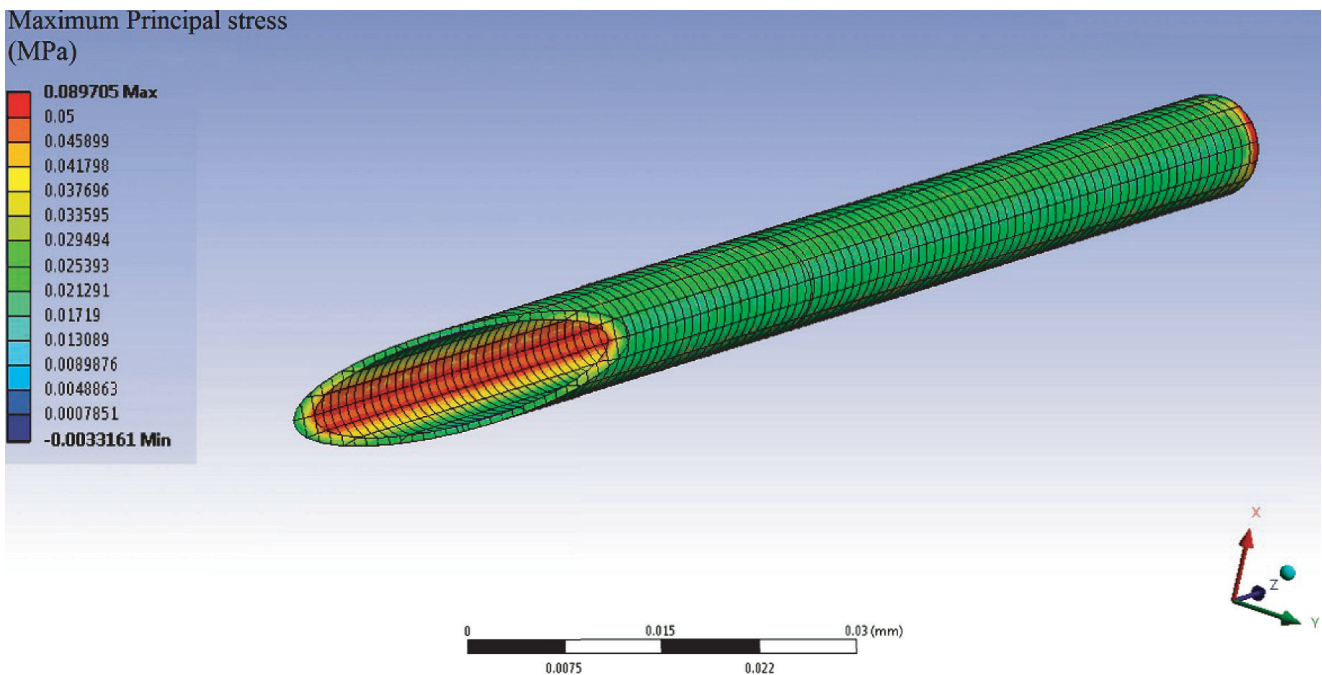


**Figure 5:** Maximum principal stresses in the capillary wall embedded in the third-level sub-model due to deformation of the global model at time  $t = 0.044$  s.

## References

- [1] H. Abe, K. Hayashi, and M. Sato, eds., *Data Book on Mechanical Properties of Living Cells, Tissues and Organs*, Springer-Verlag, New York, 1996.
- [2] B. A. Akbarnia and R. M. Campbell, *The role of the orthopaedic surgeon in child abuse*, in Lovell and Winter's Pediatric Orthopaedics, R. T. Morrissy and S. L. Weinstein, eds., Lippincott Williams and Wilkins, Philadelphia, PA, 5th ed., 2001, 1423–1445.
- [3] M. K. Bansal, S. Maraj, D. Chewaproug, and A. Amanullah, *Myocardial contusion injury: redefining the diagnostic algorithm*, *Emerg Med J*, 22 (2005), 465–469.
- [4] D. M. Cullinane and T. A. Einhorn, *Biomechanics of bone*, in Principles of Bone Biology, J. Bilezikian, L. Raisz, and G. Rodan, eds., Academic Press, San Diego, CA, 2002, 17–32.
- [5] A. Delalleau, G. Josse, J. M. Lagarde, H. Zahouani, and J. M. Bergheau, *Characterization of the mechanical properties of skin by inverse analysis combined with the indentation test*, *J Biomech*, 39 (2006), 1603–1610.
- [6] G. T. Desmoulin and G. S. Anderson, *Method to investigate contusion mechanics in living humans*, *J Forensic Biomech*, 2 (2011), Article ID F100402.
- [7] F. D. Dunstan, Z. E. Guildea, K. Kontos, A. M. Kemp, and J. R. Sibert, *A scoring system for bruise patterns: a tool for identifying abuse*, *Arch Dis Child*, 86 (2002), 330–333.
- [8] H. M. Huang, M. C. Lee, S. Y. Lee, W. T. Chiu, L. C. Pan, and C. T. Chen, *Finite element analysis of brain contusion: an indirect impact study*, *Med Biol Eng Comput*, 38 (2000), 253–259.
- [9] S. Maguire, M. K. Mann, J. Sibert, and A. Kemp, *Are there patterns of bruising in childhood which are diagnostic or suggestive of abuse? A systematic review*, *Arch Dis Child*, 90 (2005), 182–186.
- [10] A. B. Mathur, A. M. Collinsworth, W. M. Reichert, W. E. Kraus, and G. A. Truskey, *Endothelial, cardiac muscle and skeletal muscle exhibit different viscous and elastic properties as determined by atomic force microscopy*, *J Biomech*, 34 (2001), 1545–1553.
- [11] Mayo Clinic staff, *Bruise: First aid*. <http://www.mayoclinic.com/health/first-aid-bruise/FA00039>, 2012.
- [12] M. Nose, *A polygene network model for the complex pathological phenotypes of collagen disease*, *Pathol Int*, 61 (2011), 619–629.
- [13] C. Pailler-Mattei, S. Bec, and H. Zahouani, *In vivo measurements of the elastic mechanical properties of human skin by indentation tests*, *Med Eng Phys*, 30 (2008), 599–606.
- [14] Z. Puthuchear, J. R. Skipworth, J. Rawal, M. Loosemore, K. Van Someren, and H. E. Montgomery, *Genetic influences in sport and physical performance*, *Sports Med*, 41 (2011), 845–859.
- [15] M. Radmacher, M. Fritz, C. M. Kacher, J. P. Cleveland, and P. K. Hansma, *Measuring the viscoelastic properties of human platelets with the atomic force microscope*, *Biophys J*, 70 (1996), 556–567.
- [16] K. Raghavendran, B. A. Davidson, J. D. Helinski, C. J. Marschke, P. Manderscheid, J. A. Woytash, et al., *A rat model for isolated bilateral lung contusion from blunt chest trauma*, *Anesth Analg*, 101 (2005), 1482–1489.
- [17] J. D. Stitzel, F. S. Gayzik, J. J. Hoth, J. Mercier, H. D. Gage, K. A. Morton, et al., *Development of a finite element-based injury metric for pulmonary contusion part I: model development and validation*, *Stapp Car Crash J*, 49 (2005), 271–289.
- [18] J. Su, H. Zou, and T. Guo, *The study of mechanical properties on soft tissue of human forearm in vivo*, in The 3rd International Conference on Bioinformatics and Biomedical Engineering, Beijing, China, 2009, 1–4.
- [19] L. M. Tham, H. P. Lee, and C. Lu, *Cupping: from a biomechanical perspective*, *J Biomech*, 39 (2006), 2183–2193.
- [20] J. B. West, *Invited review: pulmonary capillary stress failure*, *J Appl Physiol*, 89 (2000), 2483–2489.
- [21] O. C. Zienkiewicz, R. L. Taylor, and J. Z. Zhu, *The Finite Element Method: Its Basis and Fundamentals*, Butterworth-Heinemann Publishers, Oxford, 6th ed., 2005.